Star-Shaped Oligofluorenes End-Capped with Carboxylic Groups: Syntheses and Self-Assembly at the Liquid–Solid Interface

Zhun Ma,[†] Yan-Yan Wang,[†] Pei Wang,[†] Wei Huang,[†,‡,]* Yi-Bao Li,[§,#] Sheng-Bin Lei,[§] Yan-Lian Yang,[§] Xiao-Lin Fan,[#] and Chen Wang[§,]*

[†]Institute of Advanced Materials, Fudan University, Shanghai 200433, China, [‡]Institute of Advanced Materials, Nanjing University of Posts and Telecommunications, Nanjing 210003, China, [§]National Center of Nanoscience and Technology, Beijing 100080, China, and [#]College of Chemistry and Life Science, Gannan Normal University, Jiangxi 341000, China

ABSTRACT A series of star-shaped oligofluorenes end-capped with carboxylic acid groups were synthesized. Different numbers of carboxyl groups that can form hydrogen bonds, and long alkane chains that have stabilizing effects, were intentionally introduced. The resulting molecular architectures of the so-prepared star-shaped oligofluorenes at the liquid–solid interface were investigated by scanning tunneling microscopy. It is found that the number of hydrogen-bonding groups and the symmetry of the target molecules have crucial influences on the structures of the ordered assemblies.

*Address correspondence to
wei-huang@njupt.edu.cn,
wangch@nanoctr.cn.

It is widely accepted that supramolecular assemblies of well-defined π-conjugated oligomers will play a crucial role in the advancement of molecular electronic devices, since their precise chemical structure and physical properties are able to define functional properties and facilitate enhanced control over their supramolecular structure.[1–3] The properties of such devices strongly depend on the structure of the molecular assembly on a solid surface.[4,5] Therefore, a deep understanding and fine tuning of the orientation and packing of π-conjugated oligomers in a self-assembling system are indispensable for the development of future nanodevices.

Two-dimensional (2D) assemblies of functionalized organic molecules on a solid surface have been intensively investigated by scanning tunneling microscopy (STM).[6–8] A number of π-conjugated oligomers and polymers have been reported; however, most of these 2D adlayer studies are based on simple one-dimensional oligomeric chains.[9–12] Only in recent years have arrangements of more complex oligomers been investigated.[13,14]

Among those conjugated oligomers, oligofluorenes (OFs) often act as high-performance blue emitters for application in organic light-emitting diodes (OLEDs). Modification of chemical structures with different alkyl side chains and control of their morphology afford monodisperse OFs exhibiting polarized blue emission or high glass transition temperatures (T_g).[15,16] Moreover, OFs possessing a ternary symmetry confer very promising properties for nonlinear optics and electronic or optoelectronic devices.[17,18]

In the present paper, a series of star-shaped {C}$_3$-oligofluorenes (StOFs) end-capped with one, two, or three carboxylic groups (StOF-COOH$_n$, n = 1, 2, or 3) were synthesized. Hydrogen bonds induced from carboxylic acid groups were intentionally designed at the end of the arm(s) of these star-shaped molecules. The hydrogen-bonding positions of the so-prepared StOFs were similar to those of trimesic acid (TMA). The assembly of these star-shaped oligomers was revealed by STM at the liquid–solid interface. We also demonstrate that the number of end-groups has a pronounced effect on the formation of self-assembled monolayers (SAMs) and their patterns. With contributions from intermolecular hydrogen bonding, adsorbate–substrate π–π interactions, and the stabilizing effect of long side chains, each StOF-COOH$_n$ (n = 1, 2, or 3) shows a long-range ordered molecular architecture.
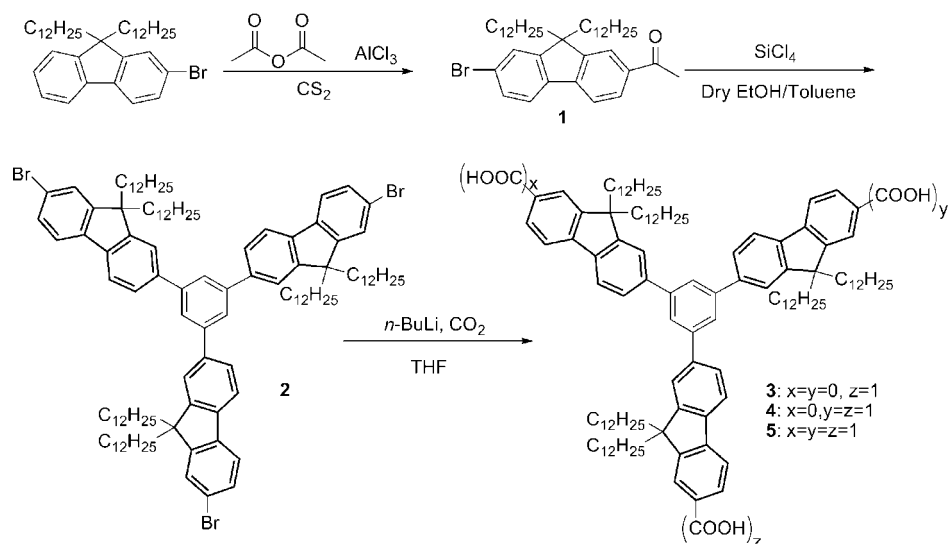
Scheme 1. Synthetic route to star-shaped oligofluorenes

RESULTS AND DISCUSSION

Oligomer Synthesis. As shown in Scheme 1, the target molecules **3**–**5** consist of three fluorene arms attached at the meta positions of a central benzenic core. 9,9-Didodecyl-2-bromo-7-acetylfluorene (**1**) was prepared according to a known procedure.[19] This compound was then cyclotrimerized via tetrachlorosilane catalysis. Pei's routes were not followed to synthesize **2** (first cyclization and second bromination);[15] on the contrary, we first acetylized 2-bromofluorene and then obtained compound **2** by direct cyclization. This modification of the reported synthetic routes increased the reaction yield and considerably reduced the difficulty of purification. Due to the active sites on the benzenic core, in Pei's reports, the StOF could not be brominated by bromine directly, so less active reagents ($Al_2O_3/CuBr_2$) were employed for bromination, but these insufficient reagents produced incomplete bromination and mono- or dibromo-substituted byproducts. The molecular weights and polarities of these byproducts were very close to those of the target compound **2**, which significantly increased the difficulties of separation and purification. However, in our cyclization reacation, nearly no byproducts existed and the yield was higher. Thin-layer chromatography (TLC) showed that there was only a small amount of reagent **1** and product **2**. These two molecules had a much greater contrast in their polarities and could be easily separated by column chromatography. The other advantage of our synthetic routes is that different numbers of carboxyl groups could be easily introduced onto StOFs in a one-step reaction from the reagent **2**, employing n-BuLi/dry ice bubbling method. Characterization of the target compounds by usual spectroscopic and analytical methods gave results in full agreement with the expected chemical structure.

Self-Assembly at the Interface. The poor coplanarity between the benzenic core and the fluorene arms in the

StOF reduces the molecule–substrate interaction. For this reason, two long alkyl chains (dodecyl) are introduced onto each fluorene moiety (position 9, sp^3 carbon) as side chains. But, when these molecules are adsorbed onto the graphite surface, only half of them have real effects on increasing the interaction between the adsorbate and highly oriented pyrolytic graphite (HOPG), because the position 9 carbon of fluorene is sp^3 hybridized (see Chart 1); therefore, only one of the dodecyl chains lies on the surface, and the other locates out from the surface. Moreover, carboxylic acid groups were introduced at the ends of this molecule, adding a molecule–molecule interaction by hydrogen bonding.

StOF-COOH₁ (3). Figure 1 shows typical STM images recorded on the StOF-COOH₁ adlayer at the octanoic acid–graphite interface. Three highly ordered domains, orientated at 120° angles relative to each other, are observed, indicating the effect of alkyl chains in the assembling process of this molecule. In each domain, the molecules align into lamellar structures. A high-resolution image indicates that the lamellae are composed by pairs of bright trigons. Each trigon is composed by three separated bright spots; the size of each spot is measured to be about 0.6 nm, and the distance between these spots is about 0.9 nm. On the basis of the chemical structure and dimension of a StOF-COOH₁ molecule, the trigons are attributed to individual molecules of **3**, and the bright spots in the trigon are attributed to fluorene moieties. The hourglass shape comprising a pair of trigons is assigned to a dimer of molecules of **3**, connected by hydrogen bonds between the carboxyl
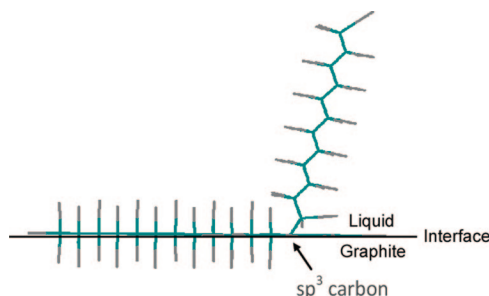

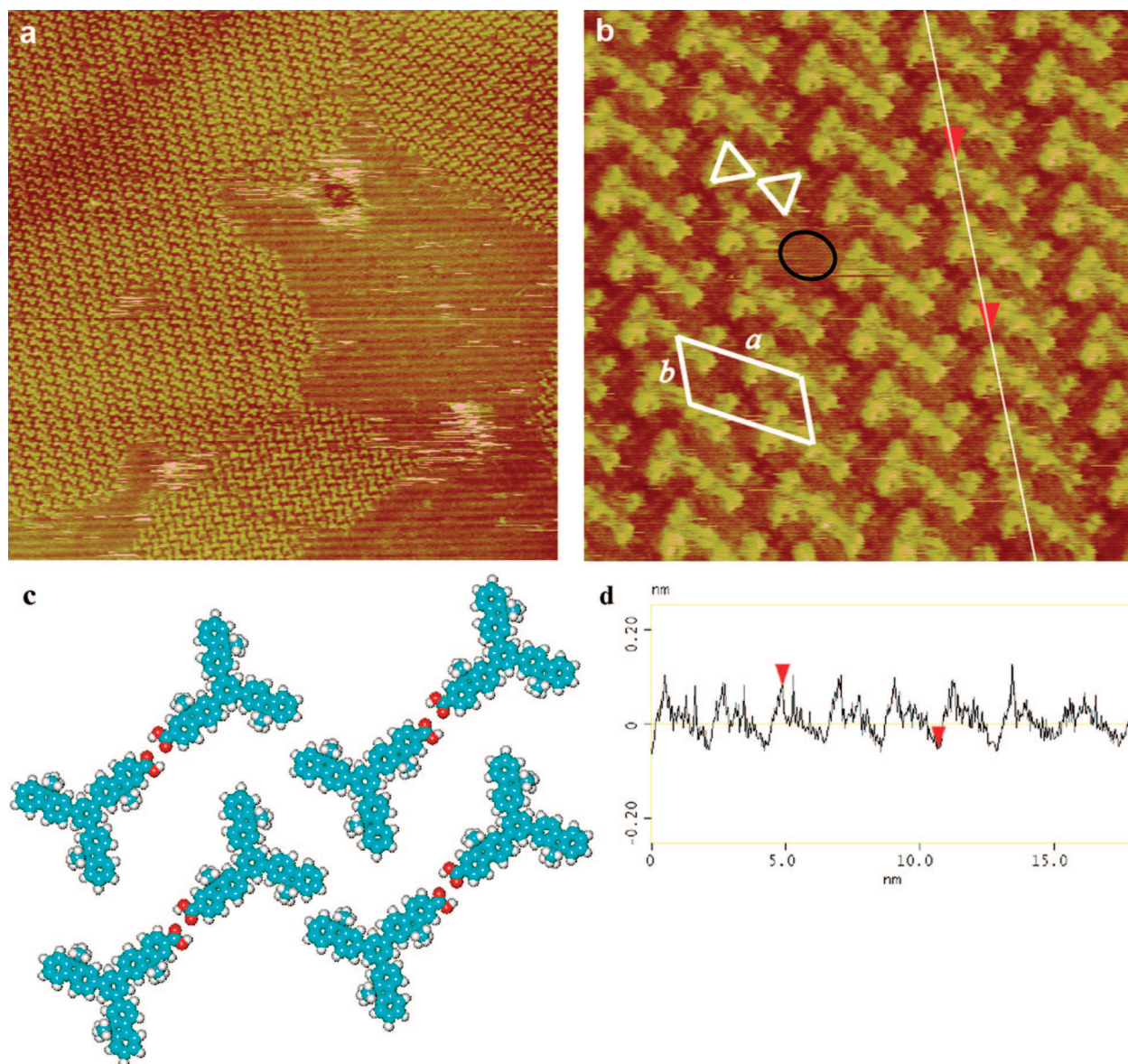Chart 1. Packing style of alkyl side chains on fluorene at the interface

Figure 1. STM images of a StOF-COOH$_1$ monolayer physisorbed at the liquid (octanoic acid)–solid (HOPG) interface: (a) 125 × 125 nm^2, I_{set} = 177 pA, V_{set} = −744 mV; (b) 17.6 × 17.6 nm^2, I_{set} = 177 pA, V_{set} = −744 mV. (c) Tentative molecular model for the 2D packing. (d) Cross-sectional profile corresponding to the white solid line in (b).

groups. The distance between these two molecules in the dimer is measured to be 2.5 nm, consistent with that of an optimized molecular dimer of **3** connected with intermolecular hydrogen bonds between carboxyl groups. The trigonal bright spots are ascribed to three fluorene arms of the molecule; in contrast, the benzene core shows a dark and unobservable feature. This may be attributed to the higher electron density on the fluorene arms and their tilted conformation from the substrate surface. A cross-sectional profile (Figure 1d) shows that the height of these bright spots is about 0.13 nm, consistent with previous observation on other aromatic moieties. Interestingly, one defect is observed where a molecule is missing, as marked in the image with an oval, but this does not influence the symmetrical molecular arrangements. According to the molecular orientation and adlayer symmetry, a unit cell is

marked in the Figure 1b, where the unit cell parameters are measured to be a = 4.2 ± 0.1 nm and b = 2.5 ± 0.1 nm, respectively. The angle α between a and b is 61 ± 1°. A structural model for the two-dimensional packing of molecules of **3** is proposed in Figure 1c. Two StOF-COOH$_1$ molecules first connect with each other through hydrogen bonds between carboxyl groups to form a dimer and then organize into stripes by the weak interactions between the side chains. Though the orientation and position of the alkyl chains could not be determined directly from the STM images, possibly due to their mobility at the interface, we believe half of them are adsorbed onto the surface and contribute to the immobilization and organization of the molecule, deduced from the distance between the molecular dimer and the area each molecule occupies
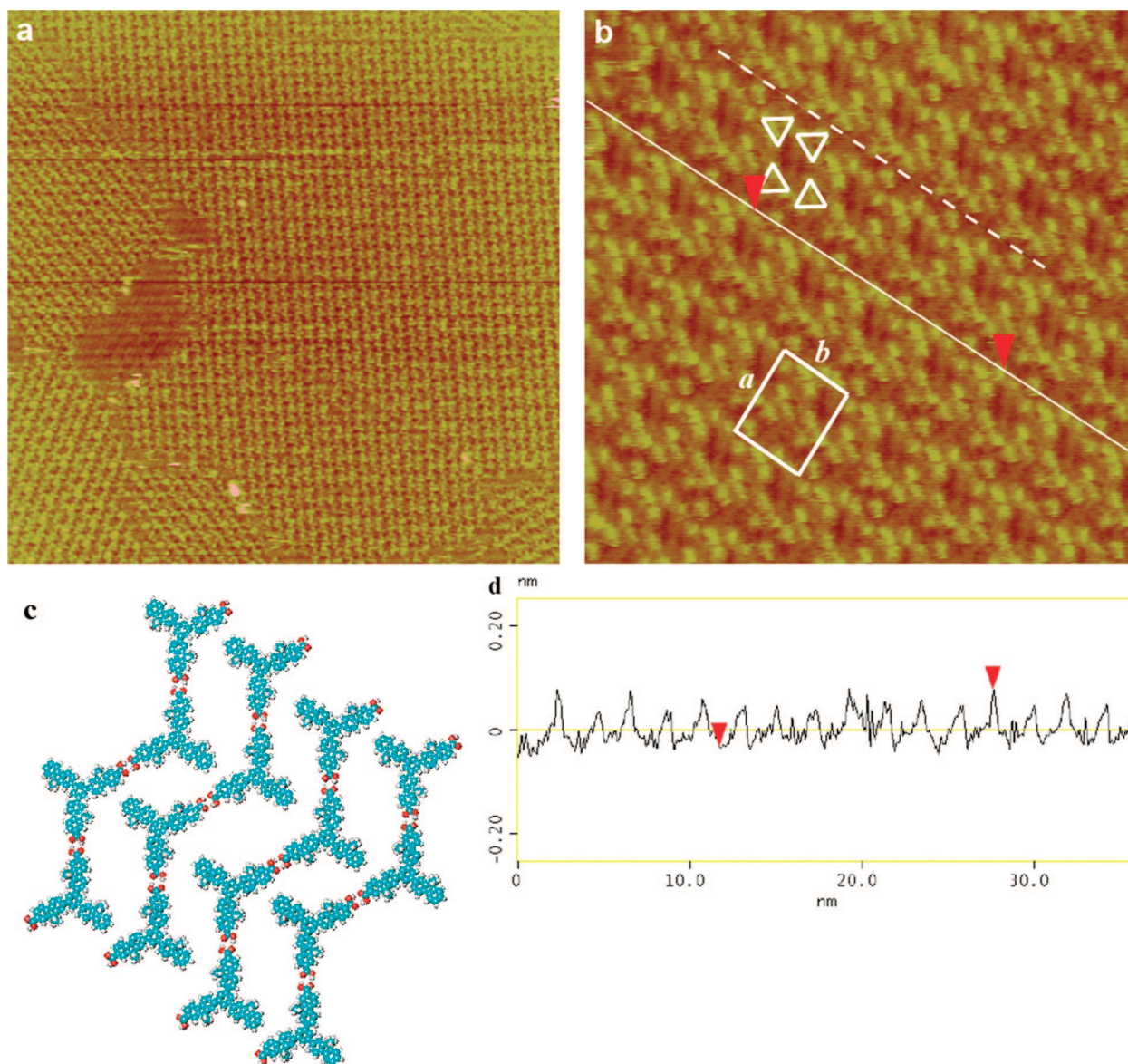
Figure 2. STM images of a StOF-COOH$_2$ monolayer physisorbed at the liquid (octanoic acid)–solid (HOPG) interface: (a) 119 × 119 nm^2, I_{set} = 171 pA, V_{set} = −792 mV; (b) 30.4 × 30.4 nm^2, I_{set} = 173 pA, V_{set} = −804 mV. (c) Tentative molecular model for the 2D packing. (d) Cross-sectional profile corresponding to the white solid line in (b).

on the surface. However, in the model, all the alkyl chains are omitted to avoid misunderstanding.

StOF-COOH$_2$ (4). With two carboxylic acid groups, compound **4** is expected to display stronger intermolecular interactions and is expected to form 2D molecular networks at the interface.

Figure 2a shows a STM image of the graphite surface after adsorption of compound **4** in octanoic acid. A long-range ordering can be clearly seen in the image, and even in a scanning area of 120 × 120 nm^2, a molecule of **4** covers nearly the whole surface and only several small defects can be found. After analyzing more than 20 images for this sample and comparing them with those of **3**, we conclude that the assembling monolayer of compound **4** has more surface coverage than compound **3**, due to the stronger interactions be-

tween molecules of compound **4**. Figure 2b is a high-resolution STM image. In this image, each molecule of **4** is also shaped like a trigon, with three separate bright spots, and an hourglass (dimer) is composed of these two trigons. This is quite similar with the adsorption pattern of compound **3**. Figure 2d shows that the height of the bright spots of one trigon is measured to be 0.11 nm, also similar to that observed for compound **3**. However, no clear lamellae formation has been observed for this molecule; instead a 2D network has been formed. Careful observation also reveals that the dimers (indicated in the image as two opposite triangles) shift by different distances with respect the two neighboring dimers. The molecular dimer marked by two opposite triangles shifts by about 1.5 nm with respect to the one on its left, while it shifts only about 0.5 nm with re-

spect to the one on its right. On the basis of this observation, a unit cell is marked in Figure 2b. According to this unit cell, four molecules are included in each unit cell, and the parameters are measured to be $a = 5.3 \pm 0.1$ nm, $b = 4.3 \pm 0.1$ nm, and $\alpha = 86 \pm 1°$.

According to the unit cell parameters, a structural model for the 2D packing of molecules of **4** is proposed in Figure 2c. In this model, the molecules are connected by intermolecular hydrogen bonds between carboxyl groups to form zigzag molecular chains. These zigzag chains shift with respect to each other to allow close packing. The molecules in the zigzag chains are connected by hydrogen bonds, while these molecular chains are only connected by van der Waals interaction, possibly between the alkyl chains. Similar to the observation with **3**, determined from the area occupied by each molecule, only half of the alkyl chains are adsorbed on the surface, and the other half point toward the solution. For the same reason as in **3**, all the alkyl chains are omitted in the model.

StOF-COOH₃ (5). This molecule is an analogue to the widely investigated TMA and its derivatives, which are capable of forming surface nanoporous networks to act as hosts in the construction of host–guest architectures. It is now of interest to further explore molecules that have structures similar to that of TMA and behave like TMA but are of different sizes in order to tune the lattice parameters and size of the cavities in the host system.[20–22] Figure 3 shows ordered domains of **5** at the octanoic acid–graphite interface. Some defects and many boundaries of domains can be discerned from a large-scale STM image. At the boundaries, the molecules are staggered and undergo more close packing (marked by ellipses, respectively). Although each ordered domain is not large, their honeycomb networks are very clear and cover nearly all the surface in our observations. In panels b and f of Figure 3, trigons shaped by three separated bright spots with a height of 0.15 nm, the same as observed for molecules **3** and **4**, fabricate honeycomb networks by linking six molecules in a circular pattern *via* hydrogen bonding. All the carboxyl groups on molecule **5** participate in hydrogen bonding by normal dimeric pairing (honeycomb). No hybrid combination of dimeric and trimeric associations (flower pattern) is revealed, which exists in certain TMA adlayers.[23] A unit cell is determined for the adlayer. The parameters of the unit cell, measured from Figure 3b, are $a = 4.4 \pm 0.1$ nm, $b = 4.2 \pm 0.1$ nm, and $\alpha = 59 \pm 1°$.

As mentioned above, the StOFs adsorb with the molecular plane parallel to the surface and only half of the alkyl chains in contact with the substrate. Thus, there exist two possibilities: a molecule adsorbs with either of its two planes toward the surface. Due to the symmetry break when the substrate is adsorbed onto the surface, two chiral adsorption conformations are induced,

as schematically shown in Figure 3c. One question, then, is whether these two isomer phases separate to form homochiral domains or mix well and organize to form heterochiral domains. Careful inspection of the high-resolution image reveals that the cavity is, in fact, three-fold rather than six-fold symmetric, with three dimer features beside alternating edges of the honeycomb. We attribute this to the alkyl chains adsorbing on the surface. It is also worth noting that the molecular dimer composing one edge of the honeycomb is not on the same line (this has been indicated in Figure 3b). On the basis of the STM observation, two possible models are proposed, as shown in Figure 3d,e. In the first model (Figure 3d), the six molecules composing one honeycomb are all the same isomer, and the structure has six-fold symmetry. The two molecules composing one edge of the honeycomb are along the same line. In the second model, the molecules on the three alternating acmes are the same chiral isomers, but the ones on the other three acmes are different. In this model, the two molecules composing one edge of the honeycomb are slightly tilted with respect to one another, consistent with the STM observation. Thus, we consider the second model more likely to represent the real case.

In principle, the honeycomb structure formed by **5** is similar to that of the related TMA and 4,4′,4′′-benzene-1,3,5-triyltribenzoic acid systems,[24] except that the size of the cavity is much larger, reaching 4 nm; in comparison, the pore sizes for TMA and 4,4′,4′′-benzene-1,3,5-triyltribenzoic acid are about 1 and 3 nm, respectively. In fact, the cavity size formed by **5** is the largest ever reported. The stabilization of such a large porous structure is surprising since, in surface adsorption, the molecules always tend to pack closely in order to minimize the surface free energy.[25] Obviously, the solvent—octanonic acid—plays an important role in the well-ordered assembling of the honeycomb with very large voids. The prior literatures reported that alkanecarboxylic acids could form associated self-assembled structures with solute molecules by coadsorption with the solute on the solid surface and they might self-assemble themselves as well.[26–28] Nevertheless, for the current system, in no case did we observe either a coadsorption structure or a monolayer of the solvent. The assembling of solutes at the liquid–solid interface is relatively complicated, involving four modes of interaction: molecule–molecule, molecule–substrate, molecule–solvent, and solvent–substrate. In this system, the solvent offers two potential stabilizing factors. One is the hydrogen-bonding interaction between the molecule and octanonic acid, and the other is the coadsorption effect of the solvent. Herein, the latter should be more prominent, although no coadsorption was scrutinized. However, this kind of coadsorption is not a strict definition. The deposition of octanonic acid molecules on the surface has a sustentative effect for the
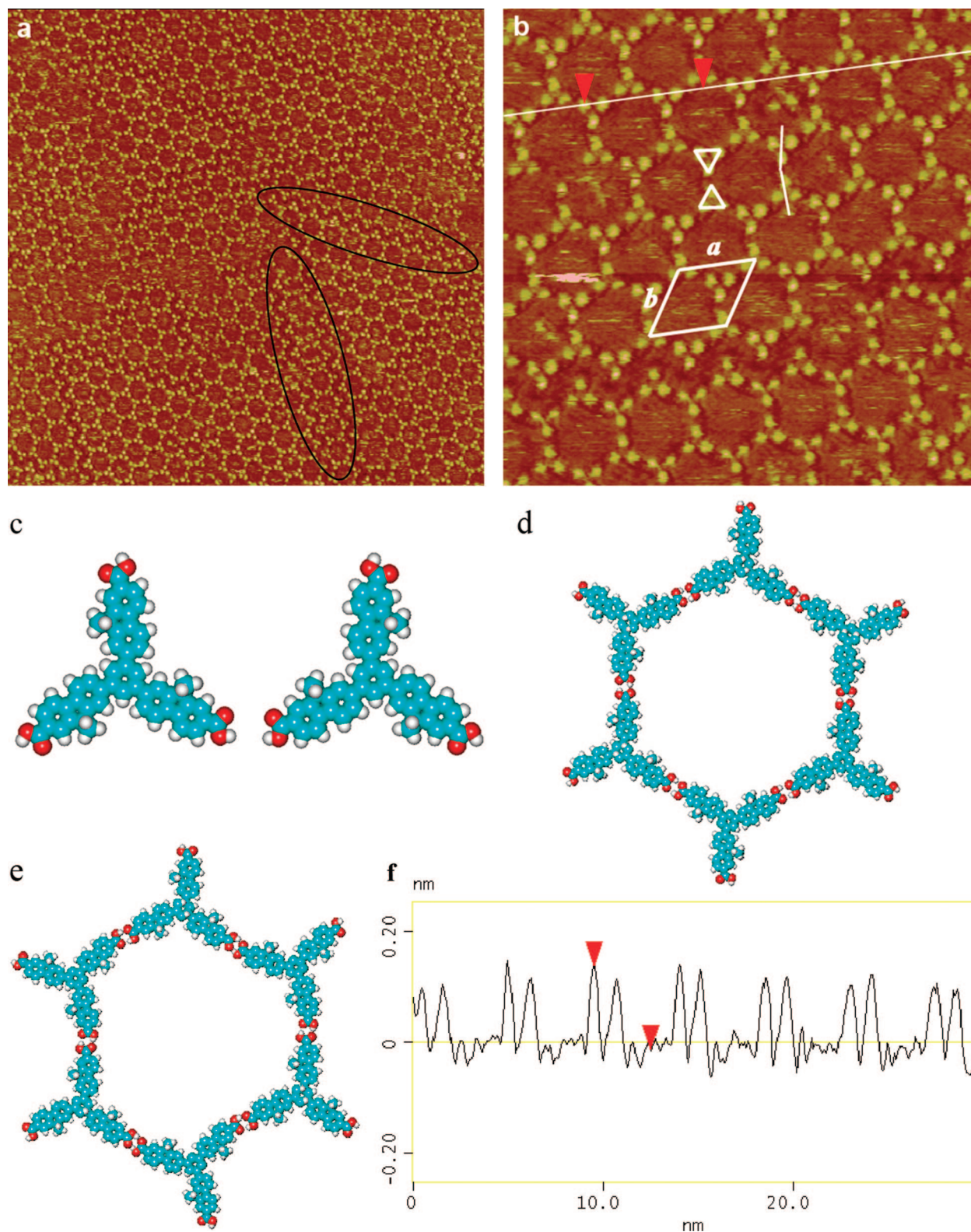
Figure 3. STM images of StOF-COOH₃ molecules physisorbed at the liquid (octanoic acid)–solid (HOPG) interface: (a) 100 × 100 nm², I_{set} = 187 pA, V_{set} = −751 mV; (b) 28.9 × 28.9 nm², I_{set} = 149 pA, V_{set} = −824 mV. (c) Molecular models for two chiral adsorption conformations of StOF-COOH₃. Two tentative molecular models for the 2D packing: (d) structures with six-fold symmetry and (e) structures with three-fold symmetry. (f) Cross-sectional profile corresponding to the white solid line in (b).

honeycomb architecture, but the molecules are possibly in poorly ordered (even discrete) and dynamic status, and thus are unable to be probed by STM. The effect and function of alkanoic acid in our system are consistent with previous reports (also, no coadsorption adlayers are observed).[29–31]

The highly porous honeycomb formed by molecules of **5** can possibly act as a host network to accept some guest molecules like coronene, fullerene, and phthalocyanine within its cavities, which embodies the concept of a host–guest system in supramolecular chemistry.[32,33] Due to the large size of the cavity, guest molecules may form molecular clusters with defined symmetry and number.[34] These programs are under investigation in our group.

CONCLUSIONS

Three star-shaped oligofluorenes with one, two, or three carboxyl terminal groups, respectively, were synthesized. STM investigation of these molecules at the octanonic acid–HOPG interface revealed that the 2D supramolecular self-assembling architectures vary with the number of carboxyl end groups, indicating the effect of symmetry and functionality of the molecules on the assembling structure. This is especially notable for StOF-COOH$_3$, which forms a hexagonal arrangement in octanonic acid, very similar to its analogue, TMA, and 4,4′,4′′-benzene-1,3,5-triyltribenzoic acid. The stabilization of the large porous structure (with cavity size reaching 4 nm) indicates that octanonic acid has a striking influence on the 2D pattern formed, stabilizing the honeycomb structure of molecules of **5** through solvent–molecule interactions and possibly "coadsorption". This hydrogen-bond-stabilized large porous network, formed by the novel star-shaped opto-electronic functional StOF-COOH$_3$, provides a suitable host template for the construction of functional host–guest architectures.

EXPERIMENTAL SECTION

Materials and Measurements. All reagents, unless otherwise specified, were obtained from Aldrich and Acros Chemical Co. and used as received. All the solvents used were further purified before use. ^{1}H NMR spectra were recorded on a Varian Mercury Plus 400 in CDCl$_3$ solution with tetramethylsilane as reference. Matrix-assisted laser desorption/ionization time-of-flight (MALDI-TOF) mass spectra were obtained using a Shimadzu AXIMA-CFR *plus* TOF mass spectrometer (Kratos Analytical, Manchester, U.K.). 2′,4′,6′-Trihydroxyacetophenone monohydrate (THAP) was selected as the matrix, and no salt was added for these conjugated oligomers. Gas chromatography–mass spectrometry (GC–MS) was performed on a Shimadzu QP-2010 instrument. The purities of the three target molecules were determined by using a Shimadzu LC-2010 high-performance liquid chromatograph (HPLC) equipped with a UV detector and an ODS column; 10 μL samples were injected into the column. Detection was performed by measuring the absorbance at 254 nm and a column temperature of 40 °C. The flow rate was set at 0.8 mL/min, and the mobile phases used were 80% CH$_3$OH and 20% CH$_3$CN.

9,9-Didodecyl-2-bromo-7-acetylfluorene (1). To a mixture of 9,9-didodecyl-2-bromo-fluorene (42 g, 77.2 mmol) and aluminum chloride (19.3 g, 144.4 mmol) in carbon disulfide was added dropwise acetic anhydride (8.1 g, 76.3 mmol) with stirring in an ice–water bath. The mixture became a bottle-green slurry and was followed to reflux for 2 h; it was then quenched by pouring into dilute hydrochloric acid. The aqueous layer was extracted by ethyl acetate. The combined extracts were washed with water, NaHCO$_3$ solution, and brine and then dried over Na$_2$SO$_4$. Removal of the solvent under vacuum, followed by column chromatography using CH$_2$Cl$_2$/petroleum ether = 3:10 as eluent, produced a yellowish solid (80%): ^{1}H NMR (CDCl$_3$, 400 MHz, ppm) 7.95 (d, 2H), 7.72 (d, 1H), 7.61 (d, 1H), 7.49 (d, 2H), 2.66 (s, 3H), 2.01–1.96 (m, 4H), 1.34–0.96 (m, 36H), 0.84 (t, 6H), 0.70 (m, 4H); GC–MS (*m/e*) 622.3 (M$^+$).

1,3,5-Tri(7-bromo-9,9-didodecylfluoren-2-yl)benzene (2). To a solution of 9,9-didodecyl-2-bromo-7-acetylfluorene (8.0 g, 12.5 mmol) in 50 mL of anhydrous ethanol/toluene (1:1) was added tetrachlorosilane (11.0 g, 65.0 mmmol) under vigorous stirring at room temperature. The mixture was then heated to reflux for 24 h. The mixture was poured into ice–water and extracted with dichloromethane. The organic phase was combined and dried over Na$_2$SO$_4$. After removal of the solvent, the product **2** was purified by column chromatography, using CH$_2$Cl$_2$/petroleum ether = 1:10 as eluent, producing a white solid (90%): ^{1}H NMR (CDCl$_3$, 400 MHz, ppm) 7.89 (s, 3H), 7.82–7.80 (d, 3H), 7.77–7.74 (d, 3H), 7.67 (s, 3H), 7.64–7.62 (d, 3H), 7.51–7.49 (m, 6H), 2.04–2.02 (m, 12H), 1.13–1.11 (m, 12H), 0.73–0.64 (m, 30H); MALDI-TOF MS (*m/e*) 1812.8 (M$^{\bullet+}$, 100%).

1-(7-Carboxyl-9,9-didodecylfluoren-2-yl)-3,5-di(9,9-didodecylfluoren-2-yl)benzene (3), 1,3-Di(7-carboxyl-9,9-didodecylfluoren-2-yl)-5-(9,9-didodecylfluoren-2-yl)benzene (4), and 1,3,5-Tri(7-carboxyl-9,9-didodecylfluoren-2-yl)benzene (5). A solution of *n*-BuLi (5.5 mL, 8.8 mmol) was added dropwise into an argon-purged solution of 1,3,5-tri(7-bromo-9,9-didodecylfluoren-2-yl)benzene (2.6 g, 1.43 mmol) in anhydrous tetrahydrofuran (20 mL) at −78 °C. The solution was then allowed to warm to room temperature with stirring for 1 h before it was cooled back to −78 °C. Carbon dioxide, dried with concentrated H$_2$SO$_4$, was bubbled into the slurry over a period of 1 h while the temperature was maintained at −78 °C. The slurry was then allowed to slowly warm to room temperature with stirring and maintained for a further 1 h before being acidified with 2 N HCl solution. The organic layer was then separated and washed with water, and the solvent was removed under reduced pressure. The crude products were purified by column chromatography, using ethyl acetate/petroleum ether = 3:10 as eluent, producing three white powders, respectively (**3**, 0.6 g, 26%; **4**, 0.76 g, 32%; **5**, 0.88 g, 36%. For **3**: ^{1}H NMR (CDCl$_3$, 400 MHz, ppm) 7.92 (d, 1H), 7.90 (s, 1H), 7.83 (d, 2H), 7.80–7.74 (m, 12H), 7.69 (s, 3H), 7.39–7.33 (m, 4H), 2.04 (m, 12H), 1.28–1.05 (m, 108H), 0.86 (t, 18H), 0.69 (m, 12H); MALDI-TOF MS (*m/e*) 1623.5 (M$^+$, 100%); purity 97.6%. For **4**: ^{1}H NMR (CDCl$_3$, 400 MHz, ppm) 8.20 (d, 2H), 8.14 (s, 2H), 7.93 (m, 6H), 7.86–7.80 (m, 6H), 7.75 (s, 3H), 7.70 (d, 1H), 7.38 (m, 2H), 2.09 (m. 12H), 1.26–1.08 (m, 108H), 0.84 (t, 18H), 0.71 (m, 12H); MALDI-TOF MS (*m/e*) 1667.2 (M$^+$, 100%); purity 96.3%. For **5**: ^{1}H NMR (CDCl$_3$, 400 MHz, ppm) 8.17 (d, 3H), 8.12 (s, 3H), 7.92 (m, 6H), 7.85–7.79 (m, 6H), 7.74 (s, 3H), 2.10 (m, 12H), 1.25–1.07 (m, 108H), 0.84 (t, 18H), 0.70 (m, 12H); MALDI-TOF MS (*m/e*) 1711.5 (M$^{\bullet+}$, 100%); purity 94.0%.

STM Characterization. The SAMs of the compounds were prepared by placing a drop (*ca*. 3 μL) of solution containing StOF-COOH$_n$ (the concentration is *ca*. 10^{-4} M) on a freshly cleaved atomically flat surface of HOPG (ZYB quality). The solvent for preparing all solutions was octanoic acid. The samples were investigated at the liquid–solid interface. A Nanoscope IIIa scanning probe microscope (Digital Instruments, Santa Barbara, CA) was employed to carry out the STM experiments using a standard constant-current mode under ambient conditions. STM tips were mechanically cut Pt/Ir wire (80/20). Experiments were repeated in several sessions using different tips to check for reproducibility and to avoid artifacts. All the STM images shown herein are presented without further processing, except flattening. The tunneling conditions used are given in the corresponding figure captions.

REFERENCES AND NOTES

1. Miura, A.; Jonkheijm, P.; De Feyter, S.; Schenning, A. P. H. J.; Meijer, E. W.; De Schryver, F. C. 2D Self-assembly of Oligo(p-phenylene vinylene) Derivatives: From Dimers to Chiral Rosettes. *Small* **2005**, *1*, 131.

2. Tour, J. M. Conjugated Macromolecules of Precise Length and Constitution. Organic Synthesis for the Construction of Nanoarchitectures. *Chem. Rev.* **1996**, *96*, 537.

3. Gong, J. R.; Zhao, J. L.; Lei, S. B.; Wan, L. J.; Bo, Z. S.; Fan, X. L.; Bai, C. L. Molecular Organization of Alkoxy-substituted Oligo(phenylene-ethynylene)s Studied by Scanning Tunneling Microscopy. *Langmuir* **2003**, *19*, 10128.

4. Bumm, L. A.; Arnold, J. J.; Cygan, M. T.; Dunbar, T. D.; Burgin, T. P.; Jones, L.; Allara, D. L.; Tour, J. M.; Weiss, P. S. Are Single Molecular Wires Conducting. *Science* **1996**, *271*, 1705.

5. Sirringhaus, H.; Brown, P. J.; Friend, R. H.; Neilsen, M. M.; Bechgaard, K.; Langeveld-Voss, B. M. W.; Spiering, A. J. H.; Janssen, R. A. J.; Meijer, E. W.; Herwig, P.; de Leeuw, D. M. Two-dimensional Charge Transport in Self-organized, High-mobility Conjugated Polymers. *Nature* **1999**, *401*, 685.

6. De Feyter, S.; De Schryver, F. C. Two-dimensional Supramolecular Self-assembly Probed by Scanning Tunneling Microscopy. *Chem. Soc. Rev.* **2003**, *32*, 139.

7. Rabe, J. P.; Buchholz, S. Commensurability and Mobility in 2-Dimensional Molecular-patterns on Graphite. *Science* **1991**, *253*, 424.

8. Mena-Osteritz, E.; Meyer, A.; Langeveld-Voss, B. M. W.; Janssen, R. A. J.; Meijer, E. W.; Bäuerle, P. Two-dimensional Crystals of Poly(3-alkylthiophene)s: Direct Visualization of Polymer Folds in Submolecular Resolution. *Angew. Chem., Int. Ed.* **2000**, *39*, 2679.

9. Lei, S. B.; Wan, L. J.; Wang, C.; Bai, C. L. Direct Observation of the Ordering and Molecular Folding of Poly[(m-phenylenevinylene)-co-(2,5-dioctoxy-p-phenylenevinylene)]. *Adv. Mater.* **2004**, *16*, 828.

10. Bäuerle, P.; Fischer, T.; Bidlingmeier, B.; Stabel, A.; Rabe, J. P. Oligothiophenes—Yet Longer—Synthesis, Characterization, and Scanning-Tunneling-Microscopy Images of Homologous, Isomerically Pure oligo(alkylthiophene)s. *Angew. Chem., Int. Ed.* **1995**, *34*, 303.

11. Gesquière, A.; Jonkheijm, P.; Schenning, A. P. H. J.; Mena-Osteritz, E.; Bauerle, P.; De Feyter, S.; De Schryver, F. C.; Meijer, E. W. Direct Observation of Chiral Oligo(p-phenylenevinylene)s with Scanning Tunneling Microscopy. *J. Mater. Chem.* **2003**, *13*, 2164.

12. Samori, P.; Yin, X.; Tchebotareva, N.; Wang, Z.; Pakula, T.; Jackel, F.; Watson, M. D.; Venturini, A.; Mullen, K.; Rabe, J. P. Self-Assembly of Electron Donor–Acceptor Dyads into Ordered Architectures in Two and Three Dimensions: Surface Patterning and Columnar "Double Cables". *J. Am. Chem. Soc.* **2004**, *126*, 3567.

13. Mahieu, G.; Grandidier, B.; Stiévenard, D.; Krzeminski, C.; Delerue, C. Adsorption Behavior of Conjugated {C}(3)-oligomers on Si(100) and Highly oriented Pyrolytic Graphite Surfaces. *Langmuir* **2003**, *19*, 3350.

14. Krömer, J.; Rios-Carreras, I.; Furhmann, G.; Musch, C.; Wunderlin, M.; Debaerdemaeker, T.; Mena-Osteritz, E.; Bauerle, P. Synthesis of the First Fully Alpha-conjugated Macrocyclic Oligothiophenes: Cyclo[n]thiophenes with Tunable Cavities in the Nanometer Regime. *Angew. Chem., Int. Ed.* **2000**, *39*, 3481.

15. Zhou, X. B.; Yan, J. C.; Pei, J. Synthesis and Relationships between the Structures and Properties of Monodisperse Star-Shaped Oligofluorenes. *Org. Lett.* **2003**, *5*, 3543.

16. Geng, Y. H.; Trajkovska, A.; Katsis, D.; Ou, J. J.; Culligan, S. W.; Chen, S. H. Synthesis, Characterization, and Optical Properties of Monodisperse Chiral Oligofluorenes. *J. Am. Chem. Soc.* **2002**, *124*, 8337.

17. Shirota, Y. Organic Materials for Electronic and Optoelectronic Devices. *J. Mater. Chem.* **2000**, *10*, 1.

18. Okumoto, K.; Shirota, Y. New Class of Hole-Blocking Amorphous Molecular Materials and Their Application in Blue-Violet-Emitting Fluorescent and Green-Emitting Phosphorescent Organic Electroluminescent Devices. *Chem. Mater.* **2003**, *15*, 699.

19. Boardman, F. H.; Dunmur, D. A.; Grossel, M. C.; Luckhurst, G. R. Synthesis and Liquid Crystal Phase Behaviour of 2-(4-Cyanophenyl)-7-n-alkylfluorenes: Luminescent Mesogens. *Chem. Lett.* **2002**, *1*, 60.

20. Lackinger, M.; Griessl, S.; Kampschulte, L.; Jamitzky, F.; Heckl, W. M. Dynamics of Grain Boundaries in Two-dimensional Hydrogen-bonded Molecular Networks. *Small* **2005**, *1*, 532.

21. Lu, J.; Zeng, Q. D.; Wang, C.; Zheng, Q. Y.; Wan, L. J.; Bai, C. L. Self-assembled Two-dimensional Hexagonal Networks. *J. Mater. Chem.* **2002**, *12*, 2856.

22. Yan, H. J.; Lu, J.; Wan, L. J.; Bai, C. L. STM Study of Two-Dimensional Assemblies of Tricarboxylic Acid Derivatives on Au(111). *J. Phys. Chem. B* **2004**, *108*, 11251.

23. Griessl, S. J. H.; Lackinger, M.; Edelwirth, M.; Hietschold, M.; Heckl, W. M. Self-assembled Two-dimensional Molecular Host-guest Architectures From Trimesic Acid. *Single Mol.* **2002**, *3*, 25.

24. Ruben, M.; Payer, D.; Landa, A.; Comisso, A.; Gattinoni, C.; Lin, N.; Collin, J. P.; Sauvage, J. P.; De Vita, A.; Kern, K. 2D Supramolecular Assemblies of Benzene-1,3,5-triyl-tribenzoic Acid: Temperature-Induced Phase Transformations and Hierarchical Organization with Macrocyclic Molecules. *J. Am. Chem. Soc.* **2006**, *128*, 15644.

25. Lei, S. B.; Wang, C.; Yin, S. X.; Wang, H. N.; Xi, F.; Liu, H. W.; Xu, B.; Wan, L. J.; Bai, C. L. Surface Stabilized Porphyrin and Phthalocyanine Two-Dimensional Network Connected by Hydrogen Bonds. *J. Phys. Chem. B* **2001**, *105*, 10838.

26. Gyarfas, B. J.; Wiggins, B.; Zosel, M. Hipps, K. W. Supramolecular Structures of Coronene and Alkane Acids at the Au(111)–Solution Interface: A Scanning Tunneling Microscopy Study. *Langmuir* **2005**, *21*, 919.

27. Tao, F.; Goswami, J.; Bernasek, S. L. Competition and Coadsorption of Di-acids and Carboxylic Acid Solvents on HOPG. *J. Phys. Chem. B* **2006**, *110*, 19562.

28. Tao, F.; Bernasek, S. L. Complexity in the Self-Assembly of Bifunctional Molecules on HOPG: The Influence of Solvent Functionality on Self-Assembled Structures. *Langmuir* **2007**, *23*, 3513.

29. Tahara, K.; Furukawa, S.; Uji-I, H.; Uchino, T.; Ichikawa, T.; Zhang, J.; Mamdouh, W.; Sonoda, M.; De Schryver, F. C.; De Feyter, S.; Tobe, Y. Two-Dimensional Porous Molecular Networks of Dehydrobenzo[12]annulene Derivatives via Alkyl Chain Interdigitation. *J. Am. Chem. Soc.* **2006**, *128*, 16613.

30. Lackinger, M.; Griessl, S.; Heckl, W. A.; Hietschold, M.; Flynn, G. W. Self-Assembly of Trimesic Acid at the Liquid–Solid Interface—A Study of Solvent-Induced Polymorphism. *Langmuir* **2005**, *21*, 4984.

31. Mamdouh, W.; Uji-I, H.; Ladislaw, J. S.; Dulcey, A. E.; Percec, V.; De Schryver, F. C.; De Feyter, S. Solvent Controlled Self-Assembly at the Liquid–Solid Interface Revealed by STM. *J. Am. Chem. Soc.* **2006**, *128*, 317.

32. Griessl, S. J. H.; Lackinger, M.; Jamitzky, F.; Markert, T.; Hietschold, M.; Heckl, W. M. Incorporation and Manipulation of Coronene in an Organic Template Structure. *Langmuir* **2004**, *20*, 9403.

33. Griessl, S. J. H.; Lackinger, M.; Jamitzky, F.; Markert, T.; Hietschold, M.; Heckl, W. M. Room-Temperature Scanning Tunneling Microscopy Manipulation of Single C-60 Molecules at the Liquid–Solid Interface: Playing Nanosoccer. *J. Phys. Chem. B* **2004**, *108*, 11556.

34. Theobald, J. A.; Oxtoby, N. S.; Phillips, M. A.; Champness, N. R.; Beton, P. H. Controlling Molecular Deposition and Layer Structure with Supramolecular Surface Assemblies. *Nature* **2003**, *424*, 1029.